Original Article

Interleukin-1 Receptor-Associated Kinase 1/4 as a Novel Target for Inhibiting Neointimal Formation After Carotid Balloon Injury

Shiru Bai[1], Dongye Li[1], Zhongmin Zhou[2], Juanli Cao[1], Tongda Xu[1], Xiaotian Zhang[1], Yi Wang[1], Jingsheng Guo[1] and Yanbin Zhang[3]

[1]Institute of Cardiovascular Disease Research, Xuzhou Medical College, Xuzhou, Jiangsu, People's Republic of China
[2]Department of Internal Medicine, Aultman Hospital & Canton Medical Education Foundation, Northeast Ohio Medical University, Canton, Ohio, USA
[3]Department of Cardiology, The Affiliated Hospital of Xuzhou Medical College, Xuzhou, Jiangsu, People's Republic of China

***Aim*: Interleukin-1 receptor-associated kinase 1 (IRAK1) and IRAK4 play essential roles in the induction of inflammatory gene products. We aimed to investigate the effect of the inhibition of IRAK1 and IRAK4 kinase activities on neointimal formation in rats with carotid artery balloon injuries using the IRAK1/4 inhibitor N-(2-Morpholinylethyl)-2-(3-nitrobenzoylamido)-benzimidazole, a cell-permeable benzimidazole compound.**

***Methods*: Wistar rats and vascular smooth muscle cells (VSMCs) isolated from the thoracic aortas were used. Toll-like receptor 4 (TLR4)-mediated nuclear factor kappa B (NFκB) signaling pathway was revealed by microarrays analysis. In addition, the differential expression of the TLR4 pathway genes, including TLR4, IRAK1, IκBα, and interleukin-1β (IL-1β), was confirmed by quantitative real-time polymerase chain reaction. Immunohistochemical staining, elastic-van Gieson and Masson staining, 5-ethynyl-2′-deoxyuridine staining, enzyme-linked immunosorbent assay, transwell migration assay and western blotting were also contributed for relevant detection.**

***Results*: The expression of TLR4 protein gradually increased at days 1, 3, 7, and 21 after balloon injury compared with the uninjured group. The dual inhibition of IRAK1 and IRAK4 attenuated neointimal formation and fibrotic remodeling after injury *in vivo* and suppressed VSMC proliferation and migration *in vitro*. The production of mediators such as tumor necrosis factor-α and IL-1β in injured arteries were also reduced by the inhibition of IRAK1 and IRAK4. The expression of NFκB p65- and F4/80-positive cells in inhibitor rats were fewer than those in control rats at day 7, while IRAK1 expression was markedly higher at day 3 in inhibitor rats. Furthermore, western blotting analysis revealed that the IRAK1/4 inhibitor suppressed the IRAK1 and IRAK4 kinase activities and the activation of the TLR4-mediated NFκB pathway *in vivo* and *in vitro*.**

***Conclusions*: This study suggested that IRAK1/4 could serve as a potential therapeutic target to suppress neointimal formation in carotid arteries after balloon injury through the TLR4/NFκB signaling pathway.**

J Atheroscler Thromb, 2015; 22: 1317-1337.

Key words: Carotid artery balloon injury, Neointimal formation, Vascular smooth muscle cell, IRAK1/4, TLR4, NFκB

Address for correspondence: Dongye Li, Institute of Cardiovascular Disease Research, Xuzhou Medical College, Xuzhou, Jiangsu, People's Republic of China
E-mail: dongyeli@yahoo.com.
Received: December 26, 2014
Accepted for publication: July 28, 2015

Introduction

Restenosis is a healing response of the arterial wall to mechanical injury after percutaneous coronary intervention (PCI). Vascular smooth muscle cell (VSMC) proliferation and migration are critical to

neointimal formation following mechanical injury. The expression of inflammatory mediators [e.g., interleukin-1 (IL-1) and tumor necrosis factor (TNF)] is triggered by vascular injury from balloon inflation or stent placement. A growing body of experimental and clinical evidence shows that inflammation drives restenosis[1, 2]. Toll-like receptor 4 (TLR4)-mediated nuclear factor kappa B (NFκB) signaling plays a crucial role in the induction of inflammatory responses in the hemorrhagic rat brain[3]. Further, the expression of TLR4 has been found to regulate VSMC proliferation related to restenosis[4], which can be upregulated by lipopolysaccharides (LPSs) in human aortic smooth muscle cells (HASMCs) in a dose- and time-dependent manner[5].

The IL-1 receptor-associated kinase (IRAK) family consists of four family members that have been identified in the human and murine genomes: IRAK1, IRAK2, IRAK3/M, and IRAK4. IRAKs are believed to mediate signal transduction from TLRs[6]. IRAK1 and IRAK4 have intrinsic serine-threonine kinase activities, whereas IRAK2 and IRAK3/M are catalytically inactive and negatively regulate TLR-mediated signaling[7-9]. All of the 11 mammalian TLRs, each of which signals to NFκB[10], with the exception of TLR3, recruit the adaptor molecule myeloid differentiation factor 88 (MyD88) through the Toll/IL-1R (TIR) domain[11].

TLR4 can be activated by cellular fibronectin, heat shock protein 60, and endogenous peptides, all of which are produced in response to tissue injury[12, 13]. Upon activation, TLR4 recruits the adaptor molecule MyD88 to their TIR domain, which in turn recruits and activates IRAK4. IRAK4 is thought to phosphorylate IRAK1, resulting in the activation and autophosphorylation of IRAK1, which can then mediate the recruitment of TNF receptor-associated factor 6 (TRAF6) to the receptor complex[14] (**Supplemental Fig. 1**) and activate two parallel TLR4-mediated signaling pathways for NFκB activation[15]. The activation of NFκB in turn induces the transcription of inflammatory cytokine and chemokine genes such as those encoding TNF-α, IL-1β, IL-6, and IL-12[16].

Kawagoe *et al.* demonstrated that the IRAK4 kinase activity plays an essential role in TLR signaling. Further, TLR-induced IRAK1/4-dependent pathways participate in the early induction of NFκB-regulated genes in response to signaling factors such as TNF-α and IκBζ[17]. However, a complete abrogation of TLR/IL-1R signaling with the use of kinase-inactive knockin mice is likely to severely impair innate immunity, which may lead to immune deficiency and dysfunctional host defense. The pharmacological inhibition of IRAK1 and IRAK4 kinase activities would be predicted to leave some degree of host defense intact while still reducing inflammatory responses[18].

A novel cell-permeable benzimidazole compound can act as a potent and selective inhibitor of IRAK1 and IRAK4 and has been tested in plasmacytoid dendritic cells from systemic lupus erythematosus and rheumatoid arthritis patients[19], human primary small airway epithelial cells in chronic obstructive pulmonary disease[20], and rat brain hypoxia/ischemia-induced neuronal injury[21]; however, it has not yet been employed in vascular research. To the best of our knowledge, there are no published studies on the role of IRAK1 and IRAK4 kinase activities in vascular restenosis through the TLR4-mediated NFκB signaling pathway. The aim of the present study was to investigate the effect of the IRAK1/4 inhibitor on neointimal formation in rat carotid arteries after balloon injury and further confirm the effect on VSMC proliferation and migration through TLR4-mediated NFκB activation.

Materials and Methods

Biological Reagents

Reagents such as 5-ethynyl-2′-deoxyuridine (EdU) and the Cell-Light™ EdU Kit were purchased from Rui Bo Guangzhou Biotechnology Limited Company (China). The elastic-van Gieson (EVG) staining reagent was purchased from Baso Zhuhai Biotechnology CO. LTD. (China). The Masson Stain Kit was bought from Nanjing Jiancheng Bioengineering Institute (China). The rat TNF-α enzyme-linked immunosorbent assay (ELISA) kit was purchased from Westang (Shanghai, China), and the rat IL-1β ELISA kit was bought from Boster (Wuhan, China). The streptavidin-peroxidase (SP) immunohistochemical assay kit, 3, 3′-diaminobenzidine (DAB) kit, and mouse anti-β-actin monoclonal antibody were purchased from Zhongshan Goldenbridge Biotechnology CO. LTD (China). Antibodies against TLR4 for western blot, IRAK4, phospho-IRAK4 (Thr345/Ser346), and phospho-IκBα (Ser32/36) were purchased from Cell Signaling Technology, Inc. (USA). The TLR4 antibody for immunohistochemistry was purchased from Bioworlde (USA). Antibodies against IRAK1, phospho-IRAK1 (Ser376), F4/80, NFκB p65, p-NFκB p65, and IκBα were purchased from Santa Cruz Biotechnology (USA).

Drug Administration

The IRAK1/4 inhibitor N-(2-Morpholinylethyl)-2-(3-nitrobenzoylamido)-benzimidazole, a cell-perme-

able benzimidazole compound that acts as a potent and selective inhibitor of IRAK1 and IRAK4, was purchased from EMD Biosciences (407601, USA). After a 25 mM (5 mg/506 μL) solution of the IRAK 1/4 inhibitor in dimethyl sulfoxide (DMSO) was prepared, it was stored at −20℃ until use. Each animal in the inhibitor group was injected intraperitoneally (i.p.) with 50 μL IRAK1/4 inhibitor per day from the day before injury until the day before euthanasia (day 21 subgroup was treated similar to day 7 subgroup). Each animal in the control group was treated with the same volume of DMSO per day. For *in vitro* experiments, the IRAK 1/4 inhibitor was further dissolved in Dulbecco's modified Eagle medium (DMEM, Hyclone, USA) with the final concentration of 1 μM[21]. The control groups were treated with the same volume of DMSO diluted in DMEM.

In vivo Studies

Animals and Experimental Groups

In total, 117 Wistar rats (male, 300−350 g) were randomly assigned to three groups: uninjured group (n=9, no operation), control group (n=60, balloon injury and intraperitoneal injection of DMSO), and inhibitor group (n=48, balloon injury and intraperitoneal injection of the IRAK1/4 inhibitor). Rats of the control and inhibitor groups were further divided into four subgroups (each subgroup n=12), which were evaluated at days 1, 3, 7, and 21 post-injury. An additional six rats each in the day 7 and 21 subgroups of the control group (n=12) were used for quantitative real-time polymerase chain reaction (qRT-PCR) analysis. All animals and forage were purchased from SLAC Laboratory Animal Limited Company (Shanghai, China). Rats were given an adequate supply of food and water. The room temperature was maintained at 23−25℃, with 50%−60% humidity and 12 h of light daily. The experimental procedure was performed in accordance with the recommendations in the Guide for the Care and Use of Laboratory Animals of the National Institutes of Health. All experiments were approved by the Animal Research Committee of Xuzhou Medical College (permit number, XMCA-CUC2010-08-114). All surgeries were performed under chloral hydrate anesthesia, and all efforts were made to minimize suffering.

Carotid Artery Balloon Injury Model in Rats

All rats were anesthetized by an intraperitoneal (i.p) injection of chloral hydrate (300 mg/kg body weight, dissolved in double-distilled water). Surgical procedures were performed using a previously described sterile surgical technique[22]. At the time of euthanasia, the left common carotid arteries were completely exposed and removed after rats were injected intraperitoneally (i.p.) with 10% chloral hydrate. Both the left and right common carotid arteries were removed for the uninjured group.

Determination of Neointimal Formation and Fibrotic Remodeling

Sections (3−5 μm thick) were stained according to the hematoxylin−eosin (H&E), EVG, and Masson staining methods. Histomorphometric analysis was performed by individuals blinded to the treatment mode. The ratio of the neointimal to medial area (N/M) was calculated using Image-Pro Plus Version 6.0 for Windows (Media Cybernetics, Inc; USA).

Evaluation of Cell Proliferation by the EdU Incorporation Method

As described in our previous study, EdU dissolved in 0.9% sodium chloride was injected i.p. into animals at a dose of 100 mg/kg 18, 12, and 2 h before euthanasia. The EdU staining was conducted according to the manufacturer's protocol as previously described[23].

Agilent Whole Genome Oligo Microarray

Total RNA from each sample was quantified using the NanoDrop ND-1000 apparatus, and the RNA integrity was assessed using standard denaturing agarose gel electrophoresis. For microarray analysis, one microgram of RNA was amplified and transcribed into fluorescent cRNA using the Quick Amp Labeling protocol (version 5.7, Agilent Technologies). The labeled cRNA were hybridized onto the Whole Rat Genome Oligo Microarray (4x44K, Agilent Technologies). After washing the slides, the arrays were scanned by the Agilent Scanner G2505B. Agilent Feature Extraction software (version 10.7.3.1) was used to analyze the acquired array images. Quantile normalization and subsequent data processing were performed using the GeneSpring GX v11.5.1 software package (Agilent Technologies). After quantile normalization of the raw data, the genes were chosen for further data analysis. Differentially expressed genes with statistical significance were identified through fold-change filtering. Pathway and GO Analysis were employed to determine the roles of these differentially expressed genes. Finally, hierarchical clustering was performed to show the distinguishable gene expression profiling among samples. Microarray data are available at http://www.ncbi.nlm.nih.gov/geo/query/acc.cgi?acc=GSE48279.

qRT-PCR Analysis

Total RNA was isolated from the frozen common carotid artery of each animal using TRIzol® reagent (Invitrogen) according to the manufacturer's instructions. The gene expression of TLR4, IRAK1, IκBα, IL-1β, and glyceraldehyde 3-phosphate dehydrogenase (GAPDH) was assayed with 2× PCR master mix (Superarray). The reaction protocol included a preincubation step at 95℃ for 10 min to activate Taq DNA polymerase, followed by 40 amplification cycles of 10 s at 95℃ and 60 s at 60℃. The results were normalized to the levels of the housekeeping gene GADPH. The primer sequences were designed using Primer 5.0 software. Specific forward and reverse primers were as follows: rat TLR4 forward: 5′-CAGGTCGAATTGTATCGCCTT-3′; rat TLR4 reverse: 5′-CCTGTGAGGTCGTTGAGGTTAG-3′; rat IRAK1 forward: 5′-GGTGGTAATACTGGAGACCCTTG-3′; rat IRAK1 reverse: 5′-AGCAGTCCAAGCATCCGTG-3′; rat IκBα forward: 5′-CGAGCATTCTATTGTGGTGATTC-3′; rat IκBα reverse: 5′-GCTACAGTCTATGGCGGTTCAA-3′; rat IL-1β forward: 5′-GAAACAGCAATGGTCGGGAC-3′; rat IL-1β reverse: 5′-TCAGAGGCAGGGAGGGAAA-3′; rat GADPH forward: 5′-GGAAAGCTGTGGCGTGAT-3′; and rat GADPH reverse: 5′-AAGGTGGAAGAATGGGAGTT-3′.

Immunohistochemical Staining for IRAK1, NFκB p65, TLR4, and F4/80

Immunohistochemical analysis was performed using the following as primary antibodies: rabbit polyclonal antibody against TLR4 (1:100), mouse monoclonal antibody against IRAK1 (1:100), rabbit polyclonal antibody against F4/80 (1:100), and rabbit polyclonal antibody against NFκB p65 (1:100). An SP immunohistochemical assay kit and a DAB kit were used during the staining procedure according to the manufacturer's instructions. F4/80-positive macrophages were counted manually and expressed as the average number of positively labeled cells per field of view (400× magnification) in the injured area.

Western Blotting Analysis

The frozen common carotid tissue was homogenized in 100 μL of ice-cold radioimmunoprecipitation (RIPA) lysis buffer including 1 μL of phenylmethylsulfonyl fluoride (PMSF) (100 mM) (Beyotime Institute of Biotechnology; China) and then incubated on ice for 30 min. Samples were centrifuged at 12,000 g for 10 min at 4℃. The supernatant was collected and measured for total protein content using the BCA Protein Assay kit (Beyotime Institute of Biotechnology, China). Thirty micrograms of total lysate was separated on sodium dodecyl sulfate (SDS)-polyacrylamide gels by electrophoresis and transferred onto polyvinylidene fluoride (PVDF) membranes. The membranes were blocked in tris-buffered saline and Tween 20 (TBST) buffer containing 5% Difco™ Skim Milk (232100, BD; USA) and incubated at 4℃ overnight with primary antibodies against the following molecules: TLR4 (1:2000), IRAK4 (1:1000), phospho-IRAK4 (1:1000), phospho-IκBα (1:1000), IRAK1 (1:200), phospho-IRAK1 (1:200), IκBα (1:200), and β-actin (1:1000). The membranes were then incubated with horseradish peroxidase (HRP)-labeled secondary antibodies at 37℃ for 2 h. Detection was performed using enhanced chemiluminescence (ECL) (Beyotime Institute of Biotechnology, China). Measurements of band density were performed using Image-Pro Plus Version 6.0 for Windows (Media Cybernetics, Inc.; USA). Each experiment was repeated three times.

Enzyme Linked Immunosorbent Assay (ELISA) for TNF-α and IL-1β

The common carotid levels of the inflammatory mediators TNF-α and IL-1β were quantified using ELISA kits specific for rats according to the manufacturers' instructions. The values were expressed as pg/μg protein.

***In vitro* Studies**

Cell Culture and Experimental Groups

VSMCs were harvested from the thoracic aortas of the Wistar rats (8−10 weeks old, 200 ± 20 g) employing the explants technique. Cells were used at passage numbers ranging from 3 to 5. VSMCs were maintained at 37℃ in DMEM containing 10% heat-inactivated fetal bovine serum (FBS, Gibco, USA) in a humidified atmosphere with 5% CO_2. The cells were serum-starved for 24 h before treatment or stimulation with reagents. To investigate the effect of IRAK1/4 inhibition on the TLR4/NFκB signaling pathway in VSMCs, LPS was employed, which can upregulate TLR4 expression and promote an inflammatory response in VSMCs[5]. In our previous study, VSMCs were stimulated with LPS from 0 to 100 μg/mL for 24 h, and we observed that VSMC proliferation was stimulated by LPS at 10 μg/mL[24]. The cultures were divided into four groups: control (no drug treatment), LPS, LPS + IRAK1/4 inhibitor, and IRAK1/4 inhibitor.

EdU Staining for VSMC Proliferation

VSMCs in the logarithmic growth phase were

seeded in 6-well plates and stimulated with LPS (10 μg/mL) in the presence or absence of the IRAK1/4 inhibitor (1 μM) for 24 h. VSMC proliferation was determined by counting the cell number. As described in our previous *in vitro* study, each well was incubated with serum-free DMEM supplemented with 500 μL EdU (50 μM) for 2 h. The EdU staining was conducted according to the manufacturer's protocol as previously described[24]. The proliferative VSMCs were represented by the EdU-positive cells.

Transwell Migration Assay

The effect of the IRAK1/4 inhibitor on VSMC migration was investigated by a modification of the Boyden chamber assay using a polycarbonate membrane filter (Corning, USA) with an 8.0 μm pore size. The membrane served as a barrier to discriminate migratory cells from non-migratory cells. After being pretreated with the IRAK1/4 inhibitor (1 μM) for 1 h, VSMCs (1×10^5 cells per well) were incubated on the Transwell apparatus and treated with LPS (10 μg/mL) and the IRAK1/4 inhibitor (1 μM) for 6 h. The cells were then fixed with 4% paraformaldehyde and stained with crystal violet solution for 10 min. The cells migrating through the membrane to the underside of the apparatus were counted manually under a microscope. The migration activity was expressed as the mean number of migratory cells in three different fields.

Western Blotting Analysis

Western blotting for the proteins from VSMCs in each group was applied using a standard protocol as described above. The following primary antibodies were used: anti-TLR4 (1:2000), anti-NFκB p65 (1:1000), anti-p-NFκB p65 (1:1000), and anti-β-actin (1:1000).

Statistical Analysis

Statistical analysis was performed using GraphPad Prism 5.0 (GraphPad Software Inc.; California, USA). All data were presented as mean ± standard error of mean (SEM). The measurements were analyzed by one-way analysis of variance (ANOVA) with subsequent Newman−Keuls multiple comparison test or by two-way analysis of variance (ANOVA), followed by Bonferroni post-tests. A difference with a P value of less than 0.05 was considered statistically significant.

Results

***In vivo* Studies**

Course of Neointimal Formation After Balloon Catheter Injury

H&E staining (**Fig. 1-A**) showed that neointimal formation was apparent at day 7, and the neointimal area was markedly increased at day 21 (0.036 ± 0.006 vs. 0.327 ± 0.029 mm^2, $P < 0.001$; **Fig. 1-B**). The medial area was significantly increased at day 3 compared with the medial area observed at day 1 and in uninjured arteries (0.189 ± 0.004 vs. 0.136 ± 0.004 mm^2, $P < 0.001$ and vs. 0.133 ± 0.004 mm^2, $P < 0.001$). Compared with day 3, the medial area was almost unchanged at day 7 ($P > 0.05$; **Fig. 1-C**). Compared with day 7, the medial area was significantly decreased at day 21 ($P < 0.05$; **Fig. 1-C**), and the N/M ratio was significantly increased at day 21 (0.189 ± 0.027 vs. 1.861 ± 0.155, $P < 0.001$; **Fig. 1-D**). H&E staining was used to identify the endothelial cells in uninjured arteries before de-endothelialization and proliferating cells in neointima, whereas EVG staining was used to better distinguish neointima and media in **Fig. 1-E**.

TLR Signaling Pathway is Involved in Neointimal Formation

To determine which signaling pathways were involved in neointimal formation, we used gene microarrays to filter out all signaling pathway genes whose expression was altered twofold in injured carotid arteries at day 7 (**Fig. 2-A**) and day 21 (**Fig. 2-B**) compared with uninjured arteries. Microarrays analysis revealed that some signaling pathways in relation to neointimal formation have changed, and the change of genes such as TLR4, IRAK1, IκBα, and IL-1β in TLR pathways was more than twofold (**Supplemental Table 1**). Therefore, we conducted this study on the TLR4/NFκB pathway in balloon injured carotid arteries. We performed qRT-PCR analysis to confirm the differential expression of the TLR4 pathway genes, including TLR4, IRAK1, IκBα, and IL-1β (**Fig. 2-C**); the results of these validation experiments were all consistent with the microarray results. The expression of TLR4 mRNA at day 7 and day 21 after injury was 1.39-fold ($P < 0.01$) and 2.13-fold ($P < 0.001$) higher in the carotid artery of balloon-injured animals than that in uninjured animals, respectively. At day 7 post-injury, IRAK1 and IκBα mRNA levels were both decreased, with transcript levels of 0.31-fold ($P < 0.001$) and 0.72-fold ($P < 0.01$) that were found in uninjured arteries, respectively. However, both transcripts recovered to the basal levels at day 21 (both $P < 0.001$). IL-1β mRNA expression levels at day 7 were elevated 1.57-fold compared with uninjured arteries ($P < 0.001$) and decreased at day 21 versus day 7 ($P < 0.01$). In **Fig. 2-D**, immunohistochemical staining analysis revealed that the expression of TLR4 gradually increased at days 1, 3, 7, and 21 after balloon injury compared with the uninjured group.

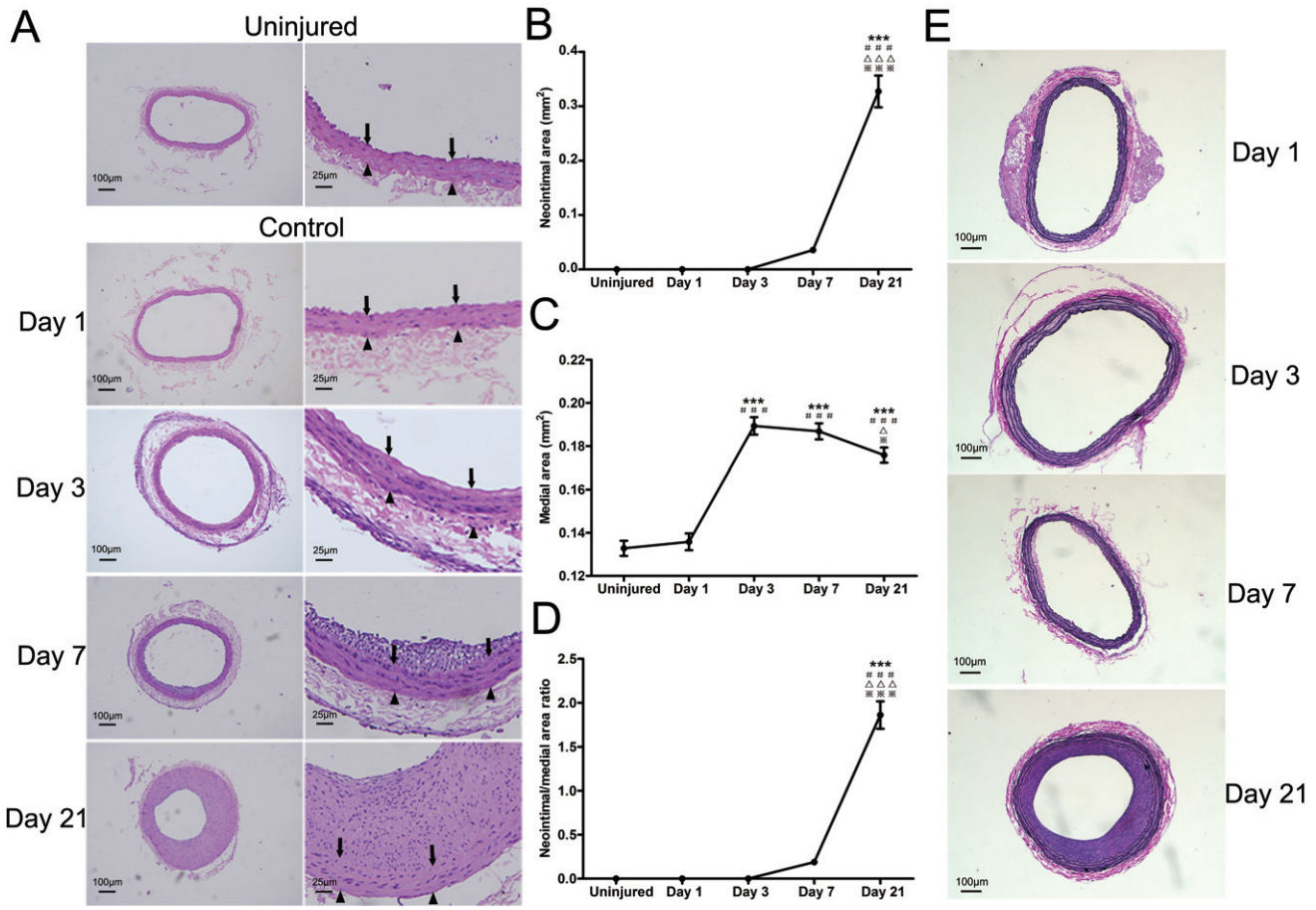

Fig. 1. Course of neointimal formation in carotid arteries after balloon injury. A) Representative H&E staining photomicrographs from uninjured arteries and injured arteries harvested at days 1, 3, 7, and 21 after denudation in the control group. Black arrows and black triangles point to the medial. B, C, and D) Line graphs represent the morphometric analysis of arterial sections for the neointimal area (mm^2), medial area (mm^2), and neointimal/medial area ratio of arteries in the uninjured and control groups. E) Representative EVG staining photomicrographs from injured arteries harvested at days 1, 3, 7, and 21 after denudation in the control group. $n=6$. ★$P<0.05$, ★★$P<0.01$, ★★★$P<0.001$ versus uninjured, #$P<0.05$, ##$P<0.05$, ###$P<0.001$ versus day 1, △$P<0.05$, △△$P<0.01$, △△△$P<0.001$ versus day 3, ※$P<0.05$, ※※$P<0.01$, ※※※$P<0.001$ versus day 7, ▲$P<0.05$, ▲▲$P<0.01$, ▲▲▲$P<0.001$ versus day 21 (All the symbols in the following graphs represent the same meaning as above).

Inhibition of IRAK1 and IRAK4 Attenuates Neointimal Formation and Fibrotic Remodeling

To further validate the relationship between neointimal formation and the TLR pathway, an IRAK1/4 inhibitor was used to observe its effect on neointimal formation, which was monitored by EVG staining (**Fig. 3-A**). As shown in **Fig. 3-B**, the neointimal area at day 21 in inhibitor-treated animals was significantly decreased compared with that of the control groups (0.182 ± 0.006 mm^2 vs. 0.326 ± 0.029, $P<0.001$); there were no significant differences at day 7 in both groups ($P>0.05$). The N/M ratio at day 21 in the inhibitor-treated rats was also significantly decreased compared with that of the control groups (1.870 ± 0.185 vs. 1.049 ± 0.015, $P<0.001$), without significant differences at day 7 in both groups ($P>0.05$; **Fig. 3-D**). Compared with the control group, the inhibition of IRAK1 and IRAK4 had no effect on the medial area at day 7 ($P>0.05$) and day 21 ($P>0.05$; **Fig. 3-C**). In **Fig. 3-E**, Masson staining showed that hyperplasia of collagen fibers was less apparent in the inhibitor group than that in the control group at days 7 and 21.

Inhibition of IRAK1 and IRAK4 Suppresses Cell Proliferation as Characterized by EdU Incorporation

To detect proliferative cells at each time point after vascular injury, animals were injected with EdU

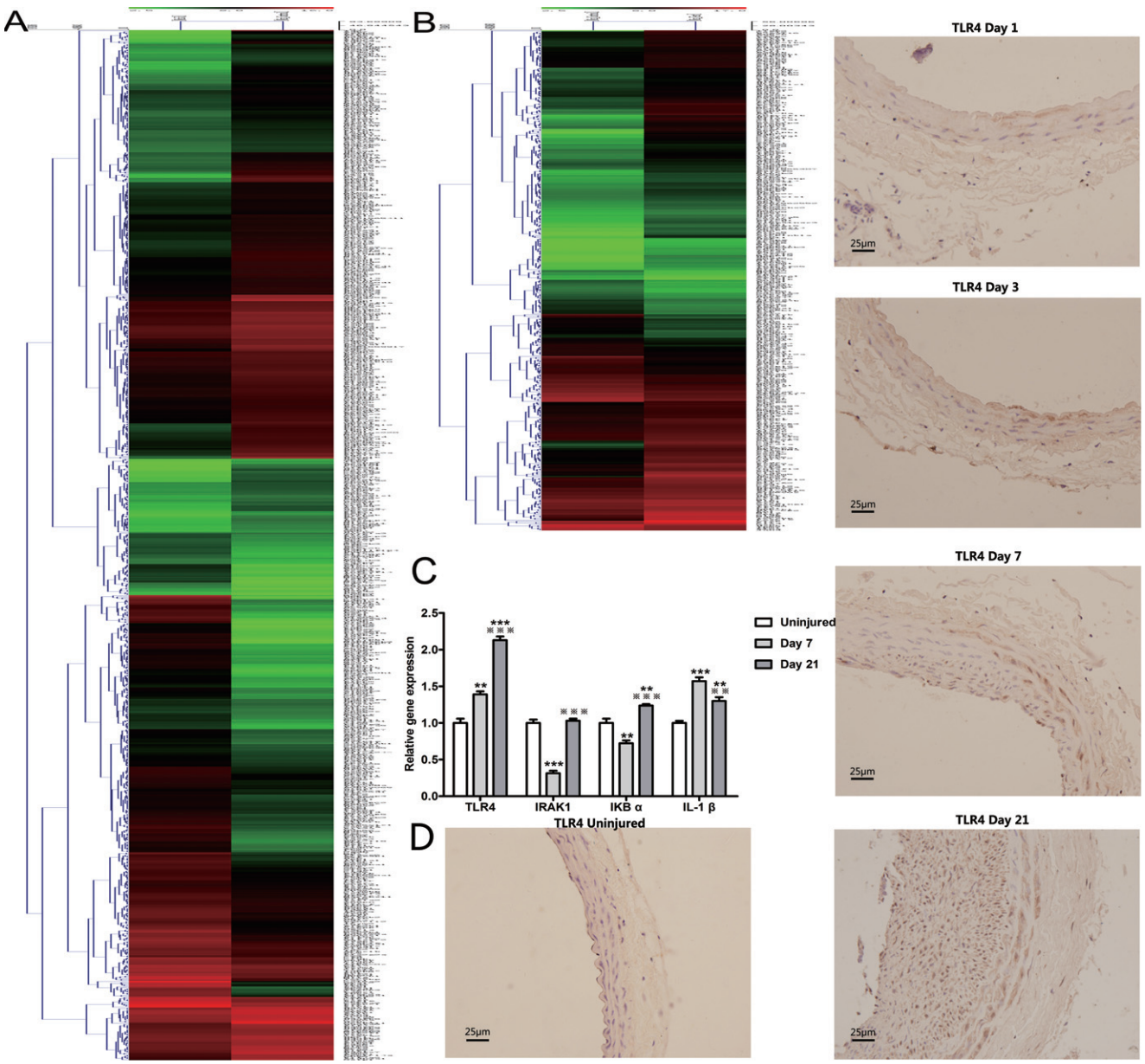

Fig. 2. mRNA and protein expression of the activated genes involved in signaling pathways including the TLR4 pathway. A and B) Heat map of the twofold changed genes involved in signaling pathways that were activated during the process of neointimal formation in balloon injured arteries at days 7 and 21 compared with the uninjured arteries, respectively. C) Quantitative real-time PCR of selected genes in the TLR4 pathway from A. The fold change was calculated compared with the expression of the uninjured group. $n=3$. D) Representative photomicrographs of immunochemical staining for TLR4 from uninjured arteries and at days 1, 3, 7, and 21 after balloon injury in the control group.

at a dose of 100 mg/kg 18, 12, and 2 h before the euthanasia procedure at days 1, 3, 7, and 21 post-injury. The EdU-positive cells percentage in the media was the highest at day 3 in control animals and was suppressed in inhibitor-treated animals (25.470 ± 2.167 vs. 14.670 ± 1.309, $P<0.001$, **Fig. 4-B**). The EdU-positive cells percentage in the media was not significantly different between the control and inhibitor groups at day 7 (5.870 ± 1.040 vs. 2.725 ± 0.599, $P>0.05$), whereas the percentage in the neointima of the inhibitor group at day 7 was significantly lower than that in the control group (82.960 ± 2.898 vs. 92.53 ± 1.679, $P<0.01$, **Fig. 4-C**). In addition, cell proliferation in injured arteries at day 1 and day 21

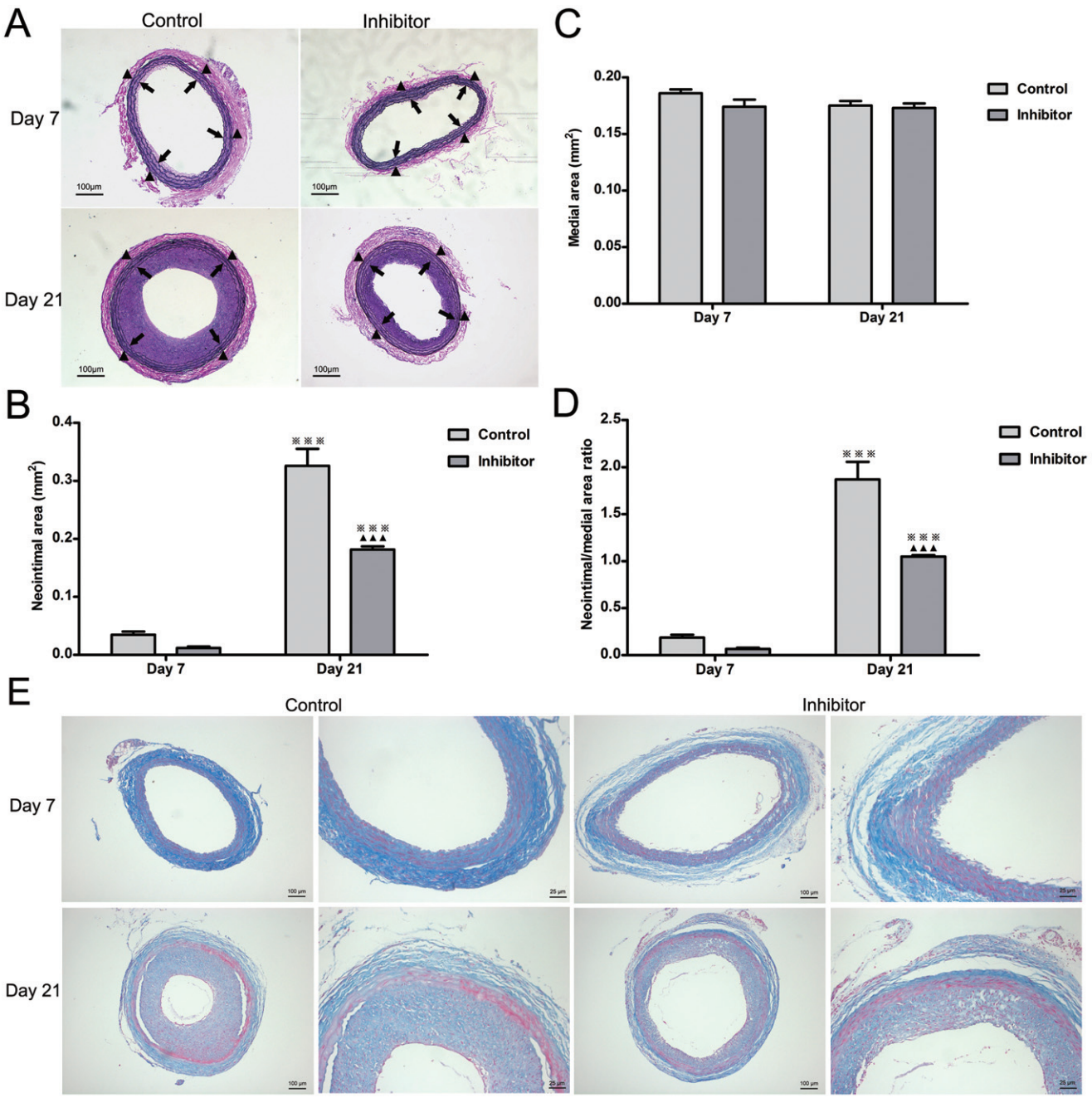

Fig. 3. Effect of the IRAK1/4 inhibitor on neointimal formation and fibrotic remodeling after injury. A) Representative photomicrographs of EVG staining from injured arteries harvested at days 7 and 21 after denudation in the control and inhibitor groups. Black arrows and black triangles point to the medial. B, C, and D) Bar graphs represent the morphometric analysis of arterial sections for the neointimal area (mm^2), medial area (mm^2), and neointimal/medial area ratio (N/M) of arteries in the control and inhibitor groups. $n=6$. E) Representative photomicrographs of Masson staining at days 7 and 21 after balloon injury in the control and inhibitor groups.

was examined by EdU staining, but almost no EdU-positive cells were observed (**Supplemental Fig. 2**).

IRAK1 and IRAK4 Kinase Activity is Attenuated by an IRAK1/4 Inhibitor

Fig. 5-A and **Fig. 5-B** show that p-IRAK1 and p-IRAK4 protein levels in the control and inhibitor

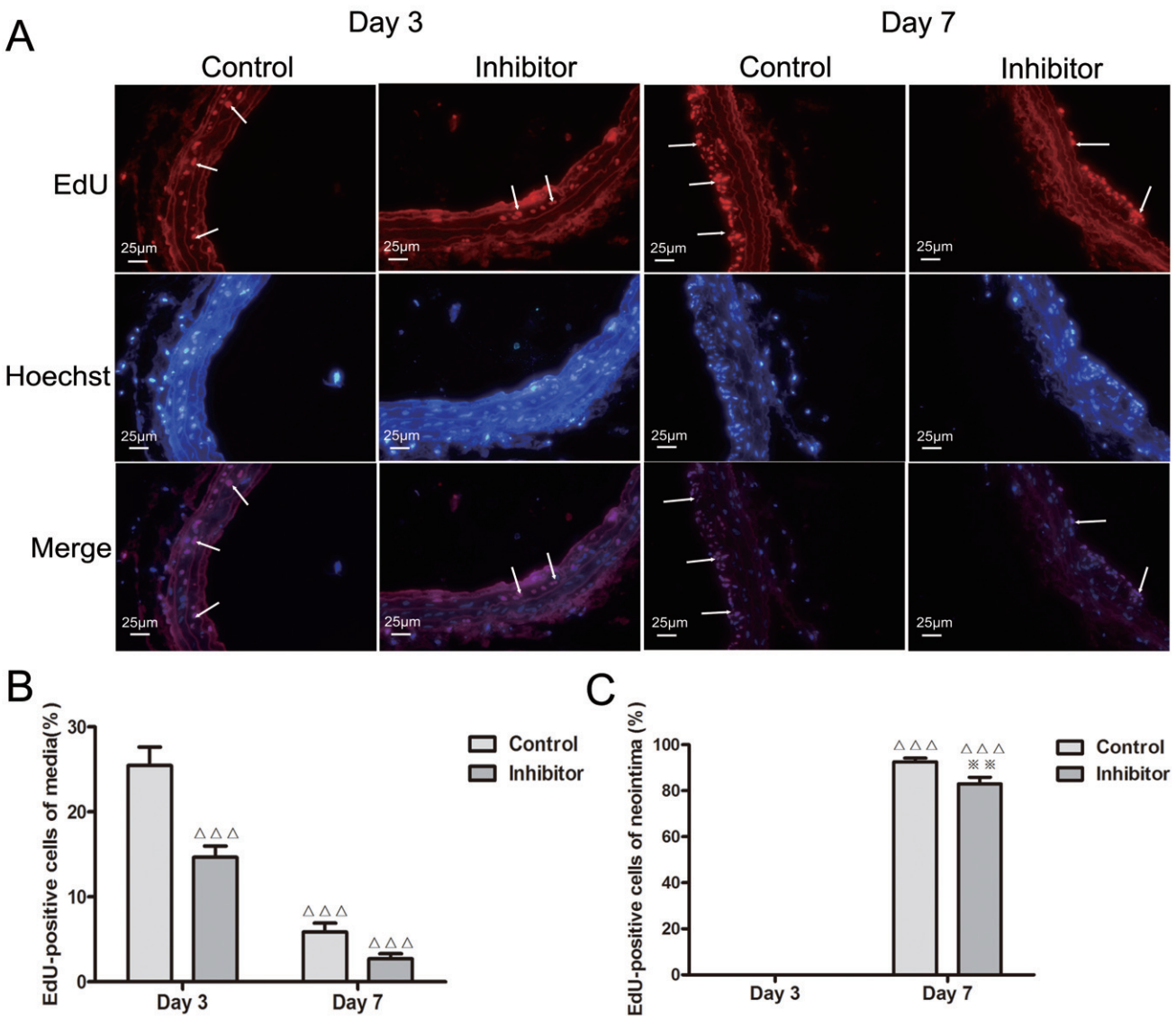

Fig. 4. IRAK1/4 inhibitor suppresses cell proliferation. A) Representative photomicrographs of EdU staining from injured arteries harvested at days 3 and 7 after balloon injury in the control and inhibitor groups. White arrows point to the EdU-positive cells. B and C) Representative photomicrographs and quantitative results of EdU staining from injured arteries harvested at days 3 and 7 after balloon injury in the control and inhibitor groups revealed that the EdU-positive cells percentage was suppressed at day 3 in the media and at day 7 in the neointima by the IRAK1/4 inhibitor. $n=4$.

groups both peaked at day 1 (1.236 ± 0.034 vs. 1.037 ± 0.035, $P<0.05$; 0.655 ± 0.056 vs. 0.473 ± 0.060, $P<0.05$, respectively) and significantly decreased at day 3 (0.619 ± 0.566 vs. 0.143 ± 0.059, $P<0.001$; 0.474 ± 0.060 vs. 0.150 ± 0.043, $P<0.001$, respectively) and day 7 (both $P>0.05$). There was a feedback upregulation of p-IRAK1 and p-IRAK4 at day 21 in both the control and inhibitor groups (0.442 ± 0.060 vs. 0.213 ± 0.059, $P<0.01$; 0.395 ± 0.042 vs. 0.227 ± 0.058, $P<0.05$, respectively).

Ubiquitination and degradation of IRAK1 and proteolytic degradation of IRAK4 following phosphorylation led to a reduced abundance of total IRAK1 and IRAK4, respectively. The inhibition of IRAK1 and IRAK4 increased the levels of IRAK4 protein (0.937 ± 0.055 vs. 1.171 ± 0.056, $P<0.05$ for day 1; 0.551 ± 0.059 vs. 0.974 ± 0.056, $P<0.001$ for day 3; 0.096 ± 0.009 vs. 0.546 ± 0.057, $P<0.001$ for day 7; 0.372 ± 0.056 vs. 0.854 ± 0.059, $P<0.001$ for day 21) by inhibiting its phosphorylation (0.655 ± 0.056 vs.

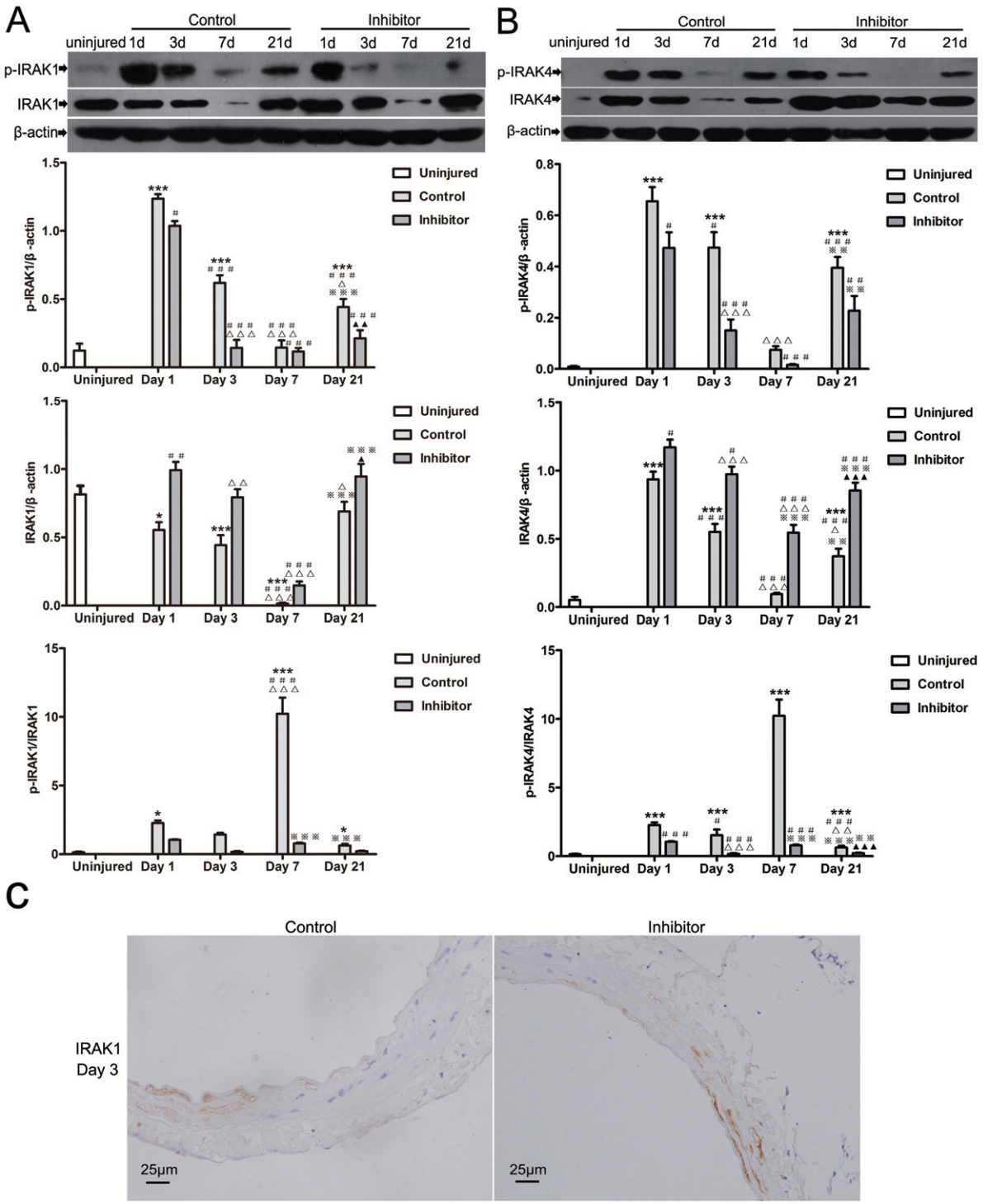

Fig. 5. IRAK1/4 inhibitor attenuates IRAK1 and IRAK4 kinase activities. A) The IRAK1/4 inhibitor lowered the levels of p-IRAK1 at days 1, 3, and 21 but not at day 7. The levels of IRAK1 protein were augmented at days 1, 3, and 21 but not at day 7. The ratio of p-IRAK1/IRAK1 at day 7 was decreased by the inhibitor. $n=3$. B) Compared with the controls, the levels of p-IRAK4 protein were inhibited at days 1, 3, and 21 but not at day 7. The inhibition of IRAK1 and IRAK4 increased the levels of IRAK4 protein at days 1, 3, 7, and 21. The ratio of p-IRAK4/IRAK4 at days 1, 3, 7, and 21 declined in the inhibitor group. $n=3$. C) Representative photomicrographs of immunochemical staining for IRAK1 from injured arteries harvested at day 3 after balloon injury in the control and inhibitor groups

0.473 ± 0.060, $P < 0.05$ for day 1; 0.474 ± 0.060 vs. 0.150 ± 0.043, $P < 0.001$ for day 3; 0.395 ± 0.042 vs. 0.227 ± 0.058, $P < 0.05$ for day 21; but $P > 0.05$ for day 7) and degradation. The ratio of p-IRAK4/IRAK4 at days 1, 3, 7, and 21 significantly declined in the inhibitor group (all $P < 0.001$) (**Fig. 5-B**). With respect to IRAK1 protein, compared with the controls, the IRAK1/4 inhibitor lowered the levels of p-IRAK1 (1.236 ± 0.034 vs. 1.037 ± 0.035, $P < 0.05$ for day 1; 0.619 ± 0.566 vs. 0.143 ± 0.059, $P < 0.001$ for day 3; 0.442 ± 0.060 vs. 0.213 ± 0.059, $P < 0.01$ for day 21; but $P > 0.05$ for day 7) and prevented the degradation of IRAK1 protein and augmented its levels at day 1 (0.554 ± 0.058 vs. 0.992 ± 0.061, $P < 0.01$), day 3 (0.443 ± 0.073 vs. 0.794 ± 0.060, $P < 0.01$), and day 21 (0.691 ± 0.070 vs. 0.946 ± 0.092, $P < 0.05$) but not day 7 ($P > 0.05$). The ratio of p-IRAK1/IRAK1 at day 7 was decreased by the inhibitor ($P < 0.001$) (**Fig. 5-A**). Immunochemical staining, shown in **Fig. 5-C**, also demonstrated that IRAK1 expression was markedly higher at day 3 in inhibitor-treated animals than that observed in control animals.

Inhibition of IRAK1 and IRAK4 Suppresses TLR4-Mediated NFκB Activation and Reduces Inflammation

As shown in **Fig. 6-A**, IRAK1 and IRAK4 inhibition suppressed the increase in TLR4 protein at day 1 (0.127 ± 0.010, $P < 0.001$), day 3 (0.370 ± 0.012, $P < 0.001$), day 7 (0.540 ± 0.013, $P < 0.001$), and day 21 (0.737 ± 0.014, $P < 0.001$). The abundance of IκBα protein is influenced by phosphorylation, ubiquitination, and degradation. As shown in **Fig. 6-B**, the inhibition of IRAK1 and IRAK4 attenuated degradation and increased the level of IκBα protein at four time points measured after injury. Simultaneously, the IRAK1/4 inhibitor suppressed the phosphorylation of IκBα. We found that p-IκBα/IκBα levels peaked at day 7 in the control and inhibitor groups and were significantly lower in the inhibitor group than those in the control group (1.839 ± 0.201 vs. 4.323 ± 0.277, $P < 0.001$).

ELISA analysis (**Fig. 6-C, D**) revealed that compared with the uninjured arteries (0.328 ± 0.041 pg/μg for IL-1β; 0.219 ± 0.018 pg/μg for TNF-α), IL-1β and TNF-α levels both peaked at day 7 (12.840 ± 0.793 pg/μg, $P < 0.001$; 8.529 ± 0.525 pg/μg, $P < 0.001$) in the control and inhibitor groups. Compared with the control group, IL-1β and TNF-α levels in inhibitor-treated animals were both significantly reduced at day 1 ($P < 0.05$; $P < 0.01$), day 3 (both $P < 0.01$), and day 7 (both $P < 0.001$). However, IRAK1/4 inhibition had no obvious effect on the production of IL-1β and TNF-α at day 21 (both $P > 0.05$). Immunohistochemical staining results showed that there were fewer F4/80-labled macrophages ($P < 0.01$) and NFκB p65-positive cells in the inhibitor group than those in the control group at day 7 (**Fig. 6-E, F** and **G**).

In vitro Studies

IRAK1/4 Inhibitor Partially Blocks LPS-Induced Proliferation and Migration of VSMC

VSMCs were stimulated by LPS (10 μg/mL) in the presence or absence of the IRAK1/4 inhibitor (1 μM) for 24 h. The results of EdU (50 μM) incorporation showed that LPS stimulated the proliferation of VSMC compared with the control group (12.550 ± 0.532 vs. 3.003 ± 0.472, $P < 0.001$), and the IRAK1/4 inhibitor reduced LPS-stimulated VSMC proliferation (9.410 ± 0.415 vs. 12.550 ± 0.532, $P < 0.001$) (**Fig. 7-A**).

The Transwell migration assay demonstrated that VSMC migration was promoted under LPS (10 μg/mL) stimulation. The number of migratory cells in the LPS group was 2.860-fold higher than that in the control group ($P < 0.001$). After being treated with the IRAK1/4 inhibitor (1 μM), LPS-stimulated VSMC migration was significantly inhibited (1.780-fold vs. 2.860-fold, $P < 0.001$) (**Fig. 7-B**).

Inhibitory Effect of the IRAK1/4 Inhibitor on VSMC through TLR4-Mediated NFκB Activation

To investigate whether the inhibitory effect of the IRAK1/4 inhibitor on VSMC proliferation and migration is associated with TLR4-mediated NFκB activation, western blotting analysis for TLR4 and NFκB was applied. As shown in **Fig. 7-C**, compared with the control group, LPS stimulated the increase of TLR4 protein expression (0.819 ± 0.022 vs. 0.445 ± 0.031, $P < 0.001$). After being treated by the IRAK1/4 inhibitor, LPS-induced TLR4 expression was suppressed (0.559 ± 0.027 vs. 0.819 ± 0.022, $P < 0.001$). This inhibitor also partially blocked LPS-induced NFκB p65 phosphorylation (1.206 ± 0.061 vs. 0.849 ± 0.085, $P < 0.01$) (**Fig. 7-D**). The results above indicated that TLR4 and NFκB activation mediated the inhibitory effect of the IRAK1/4 inhibitor on VSMC proliferation and migration stimulated by LPS.

Discussion

This study demonstrated that there was a correlative link between the signaling pathways underlying TLR4-mediated NFκB activation and cell proliferation as well as vascular inflammation. The inhibition of IRAK1 and IRAK4 kinase activity was also shown to effectively attenuate neointimal formation by sup-

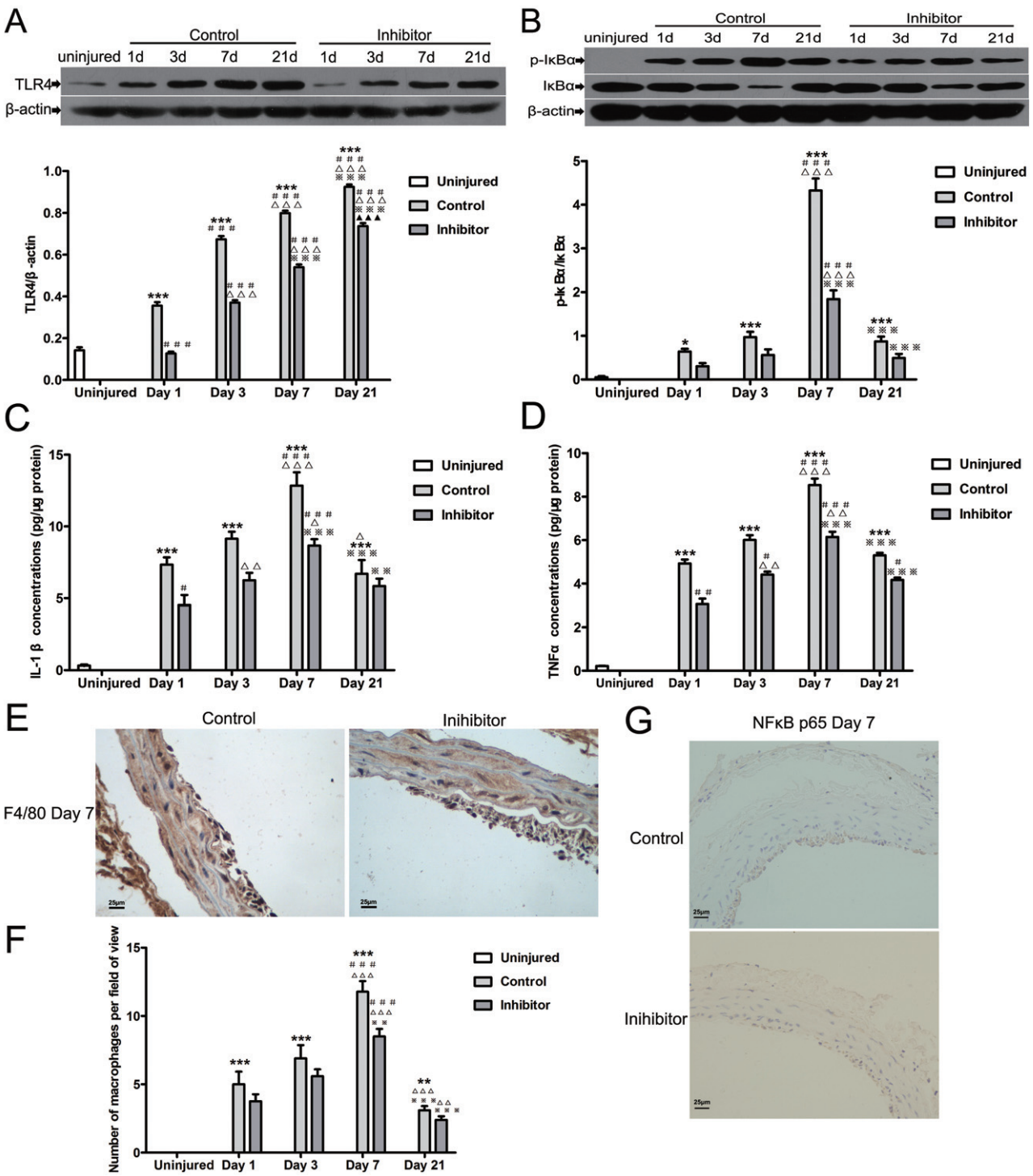

Fig. 6. IRAK1/4 inhibitor decreases TLR4-mediated NFκB activation and reduces inflammation. A) The IRAK1/4 inhibitor suppressed the increase of TLR4 protein at each time points of days 1, 3, 7, and 21. B) p-IκBα/IκBα levels were significantly lower in the inhibitor groups than that in the control groups. $n=3$. C and D) The supernatant of homogenized carotid arteries was examined for the concentrations of IL-1β and TNF-α in total protein using the rat IL-1β and TNF-α ELISA Kit, respectively. $n=3$. E and G) Representative photomicrographs of immunochemical staining for F4/80 and NFκB p65 from injured arteries at day 7 in the control and inhibitor groups, respectively. F) The number of macrophage infiltrating into injured arteries after balloon injury at days 1, 3, 7, and 21 with/without the IRAK1/4 inhibitor treatment. $n=3$.

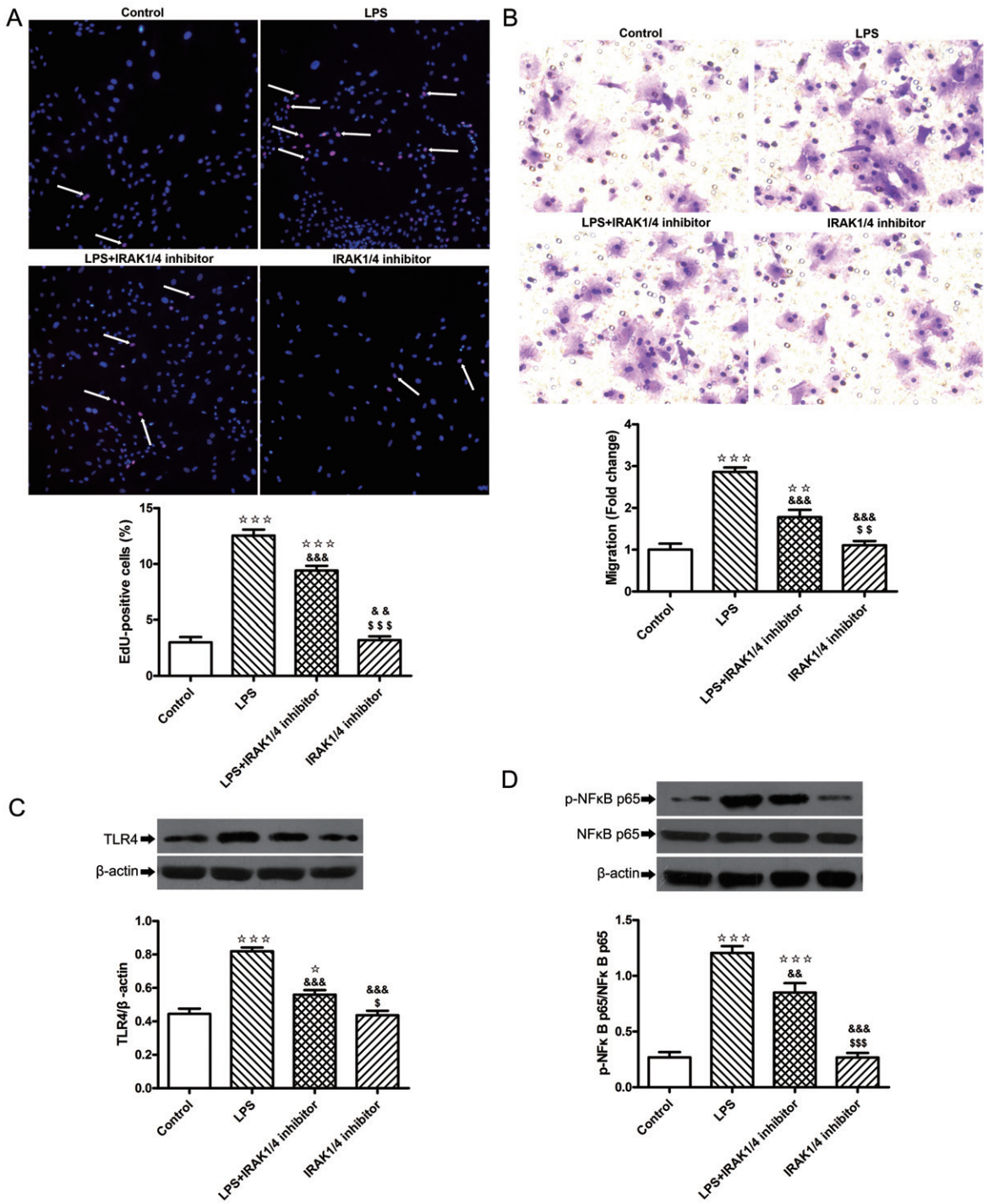

Fig. 7. IRAK1/4 inhibitor partially blocks LPS-stimulated VSMC proliferation and migration through TLR4-mediated NFκB activation. A) The IRAK1/4 inhibitor suppressed LPS-stimulated VSMC proliferation by the EdU incorporation assay. White arrows point to the EdU-positive cells. B) The Transwell migration assay showed that LPS-stimulated VSMC migration was reduced by the inhibition of IRAK1 and IRAK4. C) Compared with the control group, the levels of TLR4 protein was increased by LPS stimulation. The IRAK1/4 inhibitor partially blocked LPS-induced TLR4 expression. D) LPS stimulation activated expression of p-NFκB p65. The ratio of p-NFκB p65/NFκB p65 declined in the LPS + IRAK1/4 inhibitor group compared with that in the LPS group. ☆$P<0.05$, ☆☆$P<0.01$, ☆☆☆$P<0.001$ versus control, &&$P<0.01$, &&&$P<0.001$ versus LPS, \$$P<0.05$, \$\$$P<0.01$, \$\$\$$P<0.001$ versus LPS + IRAK1/4 inhibitor.

pressing NFκB activation.

Consistent with our previous studies[25], H&E staining showed that the neointimal area was larger beginning at day 7 after injury and progressively grew in size through day 21, whereas the medial area almost remained unchanged at day 7 and day 21 compared with that at day 3, reflecting that the migration of medial proliferative SMCs into the intima occurred after day 3. It is interesting to observe that the medial area was significantly increased at day 3 compared with that at day 1 and in uninjured arteries, which may have not generally been described in other studies of balloon injury of the rat carotid artery. We supposed that an increase of the medial area was the result of cell proliferation, which was confirmed by more EdU-positive proliferative cells in the media at day 3 than those at day 7 and day 1. Clowes *et al.* also reported that the period of maximal SMC proliferation in the media of carotid arteries after balloon injury was at day 3[26]. In this study, an obvious inhibitory effect on neointimal formation at day 21 and fibrotic remodeling at day 7 and day 21 by the IRAK1/4 inhibitor was observed.

The transcription factor NFκB is intimately involved in the early events of immune and inflammatory responses through the TLR signaling pathway[10]. NFκB is one of the pivotal regulators of proinflammatory cytokine gene expression, which has been implicated in vascular inflammation of arterial injury models[27, 28]. Upon activation, IκB is phosphorylated, ubiquitinated, and ultimately degraded by the proteosome[29]. NFκB dimers dissociate from IκB, translocate to the nucleus, and initiate the transcription of various genes involved in the immune and inflammatory responses[29], some of which (e.g., IL-1 and TNF-α) in turn activate NFκB. Thus, a positive feedback is formed between NFκB activation and the regulation of cytokine networks, and NFκB further enhances target gene expression. On the other hand, phosphorylated NFκB also initiates the transcription of the IκBα gene and promotes IκBα synthesis, and the newly synthesized IκBα inhibits the activity of NFκB[30]. The research by Bu *et al.* found that blockade of the early phase of NFκB activation in the media attenuated the expression of proinflammatory genes in the injured vessels but did not significantly affect the development of intima[27], which could explain the result that the IRAK1/4 inhibitor had no significant effect on the neointimal area at day 7. Bu *et al.* also indicated that the inhibition of the late phase of NFκB activation resulted in the downregulation of inducible nitric oxide synthase, TNF-α, and monocyte chemoattractant protein-1 expression as well as a 36% reduction in intima size[27]. An earlier study revealed that the *in vivo* transfer of NFκB decoy oligodeoxynucleotides successfully inhibited neointimal formation after balloon injury[31]. This present study revealed that treatment with an IRAK1/4 inhibitor attenuated vascular NFκB activity, which is reflected by inhibiting IκBα phosphorylation and IκBα degradation (particularly at day 7 after injury) and also by the reduced production of IL-1β and TNF-α. Immunohistochemical staining revealed that macrophage infiltration (F4/80-labled cells) and NFκB p65-positive cells in the inhibitor group were fewer than those in the control group at day 7, indicating that the accumulation of inflammatory cells could be decreased by the IRAK1/4 inhibitor. It has also been reported that the IL-1 receptor antagonist could suppress arterial inflammation, resulting in decreased neointimal formation after vascular injury[32]. In addition, the activation of NFκB p65 was verified by western blotting in LPS-stimulated VSMCs and suppressed by the IRAK1/4 inhibitor. However, its inhibitory effect on IL-1β and TNF-α production at day 21 *in vivo* was not significantly apparent, which may be due to the fact that we treated animals in the day 21 subgroup with the IRAK1/4 inhibitor for only 7 days. To obtain a stronger inhibitory effect, it may be necessary to use the inhibitor for another few days.

To investigate cell proliferation, EdU-positive cells were counted in the whole vessel wall. In the present study, an IRAK1/4 inhibitor reduced EdU-positive proliferative cells at days 3 and 7. In addition, few EdU-positive cells were observed at days 1 and 21 in both control and inhibitor-treated rats, which indicates that the cell proliferation rates were slow within 18 h before euthanasia at day 1 and day 21. One study indicated that the early decrease in IκBα protein levels and the activation of NFκB most likely reflected responses occurring in SMCs because significant numbers of macrophages were not seen in the vessel wall until day 3 after balloon denudation[28]. To explore the role of the IRAK1/4 inhibitor in the proliferation and migration of VSMCs, we conducted *in vitro* experiments with EdU incorporation and Transwell migration assay, indicating that VSMC proliferation and migration were both inhibited.

TLR4 can be activated by cellular fibronectin, which is produced in response to tissue injury[12, 13]. A rabbit endothelial denudation model found the deposition of cellular fibronectin early in the media and the adventitia and late within the luminal layers of the neointima of injured arteries[33]. The involvement of TLR4 in adventitial fibroblasts in the development of intimal lesions has also been evidenced in a mouse

femoral cuff model[34]. Consistent with the studies described above, in the present study, both TLR4 mRNA and protein levels were elevated after balloon injury to the carotid arteries and this increase persisted through day 21, suggesting that TLR4 more likely existed in medial and intimal SMCs and was activated by cellular fibronectin, contributing to neointimal formation. The *in vitro* studies also showed that a basal level of TLR4 existed in VSMCs, which was increased by LPS stimulation, and this increase could be reduced by the IRAK1/4 inhibitor. During the development of restenosis, secretory IL-1β and TNF-α from injured tissues can also promote TLR4 expression and NFκB activation as new stimulating factors. Therefore, the IRAK1/4 inhibitor reduced the production of IL-1β and TNF-α while also decreasing TLR4 expression and NFκB activation. Furthermore, the expression of TLR4 and activation of NF-κB played an important role during the transformation of macrophages to foam cells, which may accelerate the development of atherosclerosis[35]. TLR4 signaling was the mediator of chronic inflammation and an important regulator of atherogenesis[36]. Hatao *et al*. found that a prolonged stimulation of TLR2, TLR4, or TLR9 caused a decrease in IRAK4 protein accompanied by the appearance of a smaller molecular weight protein (32 kDa), which may be mediated through the cleavage of IRAK4 by a protease induced by the activation of NFκB, and the level of IRAK4 mRNA was not significantly affected[37]. In our study, the mRNA level of IRAK4 in our study was not significantly affected by balloon injury, indicating that the change in IRAK4 protein was not caused by a change at the IRAK4 mRNA level. Furthermore, qRT-PCR of IRAK4 showed that there was no significant difference between uninjured arteries and the day 7 subgroup or day 21 subgroup. We found that IRAK4 was itself overexpressed in injured arteries at day 1 and underwent phosphorylation and proteolytic degradation. A new study about the mechanism of activation for IRAK4 showed that this was an autophosphorylation that occurred by an intermolecular reaction rather than an intermolecular mechanism from another kinase[38]. Phosphorylated IRAK4 levels were diminished at days 3 and 7, following the degradation of IRAK4. Previous studies have shown that upon signal initiation, IRAK4 phosphorylated and activated IRAK1, which then resulted in the polyubiquitination and degradation of IRAK1[14]. The present study showed a high expression level of IRAK1 in uninjured arteries and gradual decreases at days 1, 3, and 7 following injury. It is intriguing that both IRAK1 and IRAK4 expression levels were elevated at day 21 and determining the mechanism responsible requires further study. The IRAK1/4 inhibitor reduced the phosphorylation and degradation of both IRAK1 and IRAK4.

IRAK4 kinase-inactive knockin mice have been studied with respect to their impaired TLR-mediated induction of proinflammatory cytokines and chemokines[39]. IRAK1-deficient mice also show dramatic impairment in IL-1R/TLR-mediated proinflammatory cytokine production[40]. Inhibition of both IRAK1 and IRAK4 is a more efficient means of blocking proinflammatory cytokine production than inhibiting either kinase alone[41]. Although the specificity of the pharmacological IRAK1 and IRAK4 inhibitors was inferior to gene knockout, Picard C *et al*. reported that IRAK4-deficient patients suffered from pyogenic bacterial infections with minimal inflammatory responses, and the human TLR-IRAK signaling pathway confers specific protection against pyogenic bacteria[39]. IRAK4 deficiency was life-threatening in infancy and childhood, with a mortality rate of 43% in their study. Most patients would have probably died in the absence of antibiotic treatment[42]. Therefore, from the viewpoint of clinical applications, the pharmacological inhibition of IRAK1 and IRAK4 kinase activities may have an advantage of retaining some degree of host defense at the time of reducing inflammatory responses. Nevertheless, we cannot rule out possible off-target and nonspecific effects of the IRAK1/4 inhibitor. For instance, it may also make a body more vulnerable to viral and bacterial infections because the TLRs mainly mediate the innate immune response by the upregulation of inflammatory cytokines in multiple cells[18]. In our study, we have observed no signs of infection in rats injected with the IRAK1/4 inhibitor. The relative axenic breeding environment for animals may be a protective factor, but this was a different case for humans. Further studies about the possible off-target and nonspecific effects need to be conducted.

In conclusion, the present study implied that the IRAK1/4 inhibitor could suppress VSMC proliferation and migration, inflammatory response, and neointimal formation through the TLR4/NFκB signaling pathway *in vitro* and *in vivo*, indicating that IRAK1/4 could serve as a potential therapeutic target to suppress neointimal formation in carotid arteries after balloon injury, which may provide a theoretical and experimental basis for the prevention and treatment of vascular restenosis following balloon angioplasty.

Acknowledgments

This work was supported by the Academic Degrees Committee and the Department of Educa-

tion of Jiangsu province (grant number CXLX11-0732). The editor and anonymous reviewers were gratefully acknowledged for the manuscript improvement.

Conflicts of Interest

The authors declare that they have no conflicts of interest.

References

1) Schillinger M, Haumer M, Schlerka G, Mlekusch W, Exner M, Ahmadi R and Minar E: Restenosis after percutaneous transluminal angioplasty in the femoropopliteal segment: the role of inflammation. J Endovasc Ther, 2001; 8: 477-483
2) Schillinger M and Minar E: Restenosis after percutaneous angioplasty: the role of vascular inflammation. Vasc Health Risk Manag, 2005; 1: 73-78
3) Teng W, Wang L, Xue W and Guan C: Activation of TLR4-mediated NFkappaB signaling in hemorrhagic brain in rats. Mediators Inflamm, 2009; 2009: 473276
4) Lin FY, Chen YH, Tasi JS, Chen JW, Yang TL, Wang HJ, Li CY, Chen YL and Lin SJ: Endotoxin induces toll-like receptor 4 expression in vascular smooth muscle cells via NADPH oxidase activation and mitogen-activated protein kinase signaling pathways. Arterioscler Thromb Vasc Biol, 2006; 26: 2630-2637
5) Li H, He Y, Zhang J, Sun S and Sun B: Lipopolysaccharide regulates toll-like receptor 4 expression in human aortic smooth muscle cells. Cell Biol Int, 2007; 31: 831-835
6) Ringwood L and Li L: The involvement of the interleukin-1 receptor-associated kinases (IRAKs) in cellular signaling networks controlling inflammation. Cytokine, 2008; 42: 1-7
7) Dunne A, Carpenter S, Brikos C, Gray P, Strelow A, Wesche H, Morrice N and O'Neill LA: IRAK1 and IRAK4 promote phosphorylation, ubiquitination, and degradation of MyD88 adaptor-like (Mal). J Biol Chem, 2010; 285: 18276-18282
8) Kobayashi K, Hernandez LD, Galan JE, Janeway CA, Jr., Medzhitov R and Flavell RA: IRAK-M is a negative regulator of Toll-like receptor signaling. Cell, 2002; 110: 191-202
9) Muzio M, Ni J, Feng P and Dixit VM: IRAK (Pelle) family member IRAK-2 and MyD88 as proximal mediators of IL-1 signaling. Science, 1997; 278: 1612-1615
10) Hayden MS and Ghosh S: Signaling to NF-kappaB. Genes Dev, 2004; 18: 2195-2224
11) Akira S, Takeda K and Kaisho T: Toll-like receptors: critical proteins linking innate and acquired immunity. Nat Immunol, 2001; 2: 675-680
12) Ohashi K, Burkart V, Flohe S and Kolb H: Cutting edge: heat shock protein 60 is a putative endogenous ligand of the toll-like receptor-4 complex. J Immunol, 2000; 164: 558-561
13) Okamura Y, Watari M, Jerud ES, Young DW, Ishizaka ST, Rose J, Chow JC and Strauss JF, 3rd: The extra domain A of fibronectin activates Toll-like receptor 4. J Biol Chem, 2001; 276: 10229-10233
14) Akira S and Takeda K: Toll-like receptor signalling. Nat Rev Immunol, 2004; 4: 499-511
15) Yao J, Kim TW, Qin J, Jiang Z, Qian Y, Xiao H, Lu Y, Qian W, Gulen MF, Sizemore N, DiDonato J, Sato S, Akira S, Su B and Li X: Interleukin-1 (IL-1)-induced TAK1-dependent Versus MEKK3-dependent NFkappaB activation pathways bifurcate at IL-1 receptor-associated kinase modification. J Biol Chem, 2007; 282: 6075-6089
16) Kawai T and Akira S: TLR signaling. Cell Death Differ, 2006; 13: 816-825
17) Kawagoe T, Sato S, Jung A, Yamamoto M, Matsui K, Kato H, Uematsu S, Takeuchi O and Akira S: Essential role of IRAK-4 protein and its kinase activity in Toll-like receptor-mediated immune responses but not in TCR signaling. J Exp Med, 2007; 204: 1013-1024
18) Li X: IRAK4 in TLR/IL-1R signaling: possible clinical applications. Eur J Immunol, 2008; 38: 614-618
19) Chiang EY, Yu X and Grogan JL: Immune complex-mediated cell activation from systemic lupus erythematosus and rheumatoid arthritis patients elaborate different requirements for IRAK1/4 kinase activity across human cell types. J Immunol, 2011; 186: 1279-1288
20) Geraghty P, Dabo AJ and D'Armiento J: TLR4 protein contributes to cigarette smoke-induced matrix metalloproteinase-1 (MMP-1) expression in chronic obstructive pulmonary disease. J Biol Chem, 2011; 286: 30211-30218
21) Yang YF, Chen Z, Hu SL, Hu J, Li B, Li JT, Wei LJ, Qian ZM, Lin JK, Feng H and Zhu G: Interleukin-1 receptor associated kinases-1/4 inhibition protects against acute hypoxia/ischemia-induced neuronal injury in vivo and in vitro. Neuroscience, 2011; 196: 25-34
22) Wang K, Zhou Z, Zhang M, Fan L, Forudi F, Zhou X, Qu W, Lincoff AM, Schmidt AM, Topol EJ and Penn MS: Peroxisome proliferator-activated receptor gamma down-regulates receptor for advanced glycation end products and inhibits smooth muscle cell proliferation in a diabetic and nondiabetic rat carotid artery injury model. J Pharmacol Exp Ther, 2006; 317: 37-43
23) Guo J, Li D, Bai S, Xu T, Zhou Z and Zhang Y: Detecting DNA synthesis of neointimal formation after catheter balloon injury in GK and in Wistar rats: using 5-ethynyl-2'-deoxyuridine. Cardiovasc Diabetol, 2012; 11: 150
24) Jiang D, Li D, Cao L, Wang L, Zhu S, Xu T, Wang C and Pan D: Positive feedback regulation of proliferation in vascular smooth muscle cells stimulated by lipopolysaccharide is mediated through the TLR 4/Rac1/Akt pathway. PLoS One, 2014; 9: e92398
25) Park SH, Marso SP, Zhou Z, Foroudi F, Topol EJ and Lincoff AM: Neointimal hyperplasia after arterial injury is increased in a rat model of non-insulin-dependent diabetes mellitus. Circulation, 2001; 104: 815-819
26) Clowes AW, Reidy MA and Clowes MM: Kinetics of cellular proliferation after arterial injury. I. Smooth muscle growth in the absence of endothelium. Lab Invest, 1983; 49: 327-333

27) Bu DX, Erl W, de Martin R, Hansson GK and Yan ZQ: IKKbeta-dependent NF-kappaB pathway controls vascular inflammation and intimal hyperplasia. FASEB J, 2005; 19: 1293-1295
28) Landry DB, Couper LL, Bryant SR and Lindner V: Activation of the NF-kappa B and I kappa B system in smooth muscle cells after rat arterial injury. Induction of vascular cell adhesion molecule-1 and monocyte chemoattractant protein-1. Am J Pathol, 1997; 151: 1085-1095
29) Karin M and Ben-Neriah Y: Phosphorylation meets ubiquitination: the control of NF-[kappa]B activity. Annu Rev Immunol, 2000; 18: 621-663
30) Hoffmann A, Levchenko A, Scott ML and Baltimore D: The IkappaB-NF-kappaB signaling module: temporal control and selective gene activation. Science, 2002; 298: 1241-1245
31) Yoshimura S, Morishita R, Hayashi K, Yamamoto K, Nakagami H, Kaneda Y, Sakai N and Ogihara T: Inhibition of intimal hyperplasia after balloon injury in rat carotid artery model using cis-element 'decoy' of nuclear factor-kappaB binding site as a novel molecular strategy. Gene Ther, 2001; 8: 1635-1642
32) Isoda K, Akita K, Isobe S, Niida T, Adachi T, Iwakura Y and Daida H: Interleukin-1 receptor antagonist originating from bone marrowderived cells and non-bone marrow-derived cells helps to suppress arterial inflammation and reduce neointimal formation after injury. J Atheroscler Thromb, 2014; 21: 1208-1218
33) Bauters C, Marotte F, Hamon M, Oliviero P, Farhadian F, Robert V, Samuel JL and Rappaport L: Accumulation of fetal fibronectin mRNAs after balloon denudation of rabbit arteries. Circulation, 1995; 92: 904-911
34) Vink A, Schoneveld AH, van der Meer JJ, van Middelaar BJ, Sluijter JP, Smeets MB, Quax PH, Lim SK, Borst C, Pasterkamp G and de Kleijn DP: In vivo evidence for a role of toll-like receptor 4 in the development of intimal lesions. Circulation, 2002; 106: 1985-1990
35) Zhang X, Xie Y, Zhou H, Xu Y, Liu J, Xie H and Yan J: Involvement of TLR4 in oxidized LDL/beta2GPI/anti-beta2GPI-induced transformation of macrophages to foam cells. J Atheroscler Thromb, 2014; 21: 1140-1151
36) Eguchi K and Manabe I: Toll-like receptor, lipotoxicity and chronic inflammation: the pathological link between obesity and cardiometabolic disease. J Atheroscler Thromb, 2014; 21: 629-639
37) Hatao F, Muroi M, Hiki N, Ogawa T, Mimura Y, Kaminishi M and Tanamoto K: Prolonged Toll-like receptor stimulation leads to down-regulation of IRAK-4 protein. J Leukoc Biol, 2004; 76: 904-908
38) Cushing L, Stochaj W, Siegel M, Czerwinski R, Dower K, Wright Q, Hirschfield M, Casanova JL, Picard C, Puel A, Lin LL and Rao V: Interleukin 1/Toll-Like receptor induced autophosphorylation activates interleukin 1 receptor-associated kinase 4 and controls cytokine induction in a cell-type specific manner. J Biol Chem, 2014; : [Epub ahead of print]
39) Picard C, Puel A, Bonnet M, Ku CL, Bustamante J, Yang K, Soudais C, Dupuis S, Feinberg J, Fieschi C, Elbim C, Hitchcock R, Lammas D, Davies G, Al-Ghonaium A, Al-Rayes H, Al-Jumaah S, Al-Hajjar S, Al-Mohsen IZ, Frayha HH, Rucker R, Hawn TR, Aderem A, Tufenkeji H, Haraguchi S, Day NK, Good RA, Gougerot-Pocidalo MA, Ozinsky A and Casanova JL: Pyogenic bacterial infections in humans with IRAK-4 deficiency. Science, 2003; 299: 2076-2079
40) Kanakaraj P, Schafer PH, Cavender DE, Wu Y, Ngo K, Grealish PF, Wadsworth SA, Peterson PA, Siekierka JJ, Harris CA and Fung-Leung WP: Interleukin (IL)-1 receptor-associated kinase (IRAK) requirement for optimal induction of multiple IL-1 signaling pathways and IL-6 production. J Exp Med, 1998; 187: 2073-2079
41) Song KW, Talamas FX, Suttmann RT, Olson PS, Barnett JW, Lee SW, Thompson KD, Jin S, Hekmat-Nejad M, Cai TZ, Manning AM, Hill RJ and Wong BR: The kinase activities of interleukin-1 receptor associated kinase (IRAK)-1 and 4 are redundant in the control of inflammatory cytokine expression in human cells. Mol Immunol, 2009; 46: 1458-1466
42) Ku CL, von Bernuth H, Picard C, Zhang SY, Chang HH, Yang K, Chrabieh M, Issekutz AC, Cunningham CK, Gallin J, Holland SM, Roifman C, Ehl S, Smart J, Tang M, Barrat FJ, Levy O, McDonald D, Day-Good NK, Miller R, Takada H, Hara T, Al-Hajjar S, Al-Ghonaium A, Speert D, Sanlaville D, Li X, Geissmann F, Vivier E, Marodi L, Garty BZ, Chapel H, Rodriguez-Gallego C, Bossuyt X, Abel L, Puel A and Casanova JL: Selective predisposition to bacterial infections in IRAK-4-deficient children: IRAK-4-dependent TLRs are otherwise redundant in protective immunity. J Exp Med, 2007; 204: 2407-2422

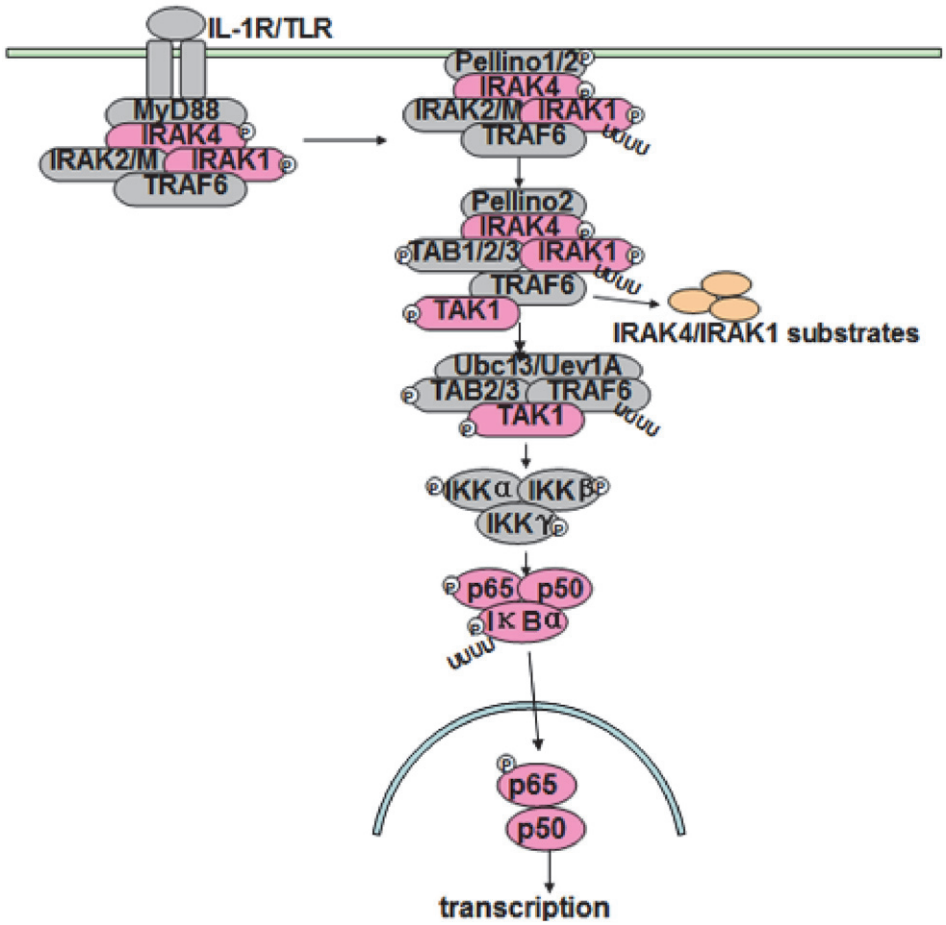

Supplemental Fig. 1.
Upon stimulation, IL-1R/TLR recruits the adaptor molecule MyD88 to their TIR domain. Sequentially, MyD88 recruits and activates IRAK4. IRAK4 is thought to phosphorylate IRAK1, resulting in the autophosphorylation of IRAK1 and the interaction with adaptor Pellino1/2, and then IRAK1 mediates the recruitment of TRAF6 to the receptor complex. TAK1 binding protein 1 (TAB1) triggers TAK1 autophosphorylation. TAB2/3 adaptor proteins link TAK1 with TRAF6 to mediate TAK1 activation. TRAF6, a RING domain protein, functions as an ubiquitin protein ligase E3. Activated TRAF6 by IRAKs form a complex with Ubc13 and Uev1A, which function as ubiquitin ligase E2. TAK1 activates the IKK complex composed of the regulatory subunit IKKγ and the catalytic subunits IKKα and IKKβ, which catalyzes IκBα phosphorylation, ubiquitination, and degradation, allowing NFκB (p65/p50) to translocate to the nucleus and activate transcription of proinflammatory cytokines.

Supplemental Table 1.
TLR signaling pathway genes only containing the TLR pathway changed genes which were selected from "Differentially Expressed Genes" (including Wistar 7d vs. Wistar uninjured, Wistar 21d vs. Wistar uninjured, twofold change)

	Wis7d vs. Wis_Uninjured 2.0 fold down/upregulated genes					
	Fold change and Regulation		Raw Intensity		Normalized Intensity	
ProbeName	Absolute Fold change [(Wis_Uninjured) vs. (Wis7d)]	Regulation [(Wis_Uninjured) vs. (Wis7d)]	[Wis_Uninjured] (raw)	[Wis7d] (raw)	[Wis_Uninjured] (normalized)	[Wis7d] (normalized)
A_44_P532352	2.3156652	down	95.82009	145.39401	8.19992	6.988493
A_43_P14911	3.1112941	up	18.216698	328.7614	5.273629	8.384923
A_44_P996124	2.3754249	up	21.297314	133.46379	5.592055	6.8402405
	Wis_21d vs. Wis_Uninjured 2.0 fold upregulated genes					
	Fold change and Regulation		Raw Intensity		Normalized Intensity	
ProbeName	Absolute Fold change [(Wis_Test) vs. (Wis_Uninjured)]	Regulation [(Wis_Test) vs. (Wis_Uninjured)]	[Wis_Uninjured] (raw)	[Wis_21d] (raw)	[Wis_Uninjured] (normalized)	[Wis_21d] (normalized)
A_44_P996124	4.393306034	up	21.297314	210.79536	5.592055	7.727362
A_44_P261450	2.130347824	up	885.71045	5158.449	11.145009	12.236098
A_43_P14911	2.0991976	up	18.2167	101.0333	5.273629	6.343467

Fold Change cut-off: 2.0
Column A: ProbeName; it represents probe name.
Column B: Absolute Fold change; the absolute ratio (no log scale) of normalized intensities between two samples.
Column C: Regulation; it depicts which one of the samples has greater or lower intensity values wrt other sample.
Column D,E: Raw Intensity of each sample.
Column F,G: log2 value of normalized intensity of each sample.
Column H−O: Annotations to each probe, including GenbankAccession, GenomicCoordinates, Description, GeneSymbol, Go, RefSeqAccession, UniGeneID, EntrezGeneID.
Example: $2^{8.19992}/2^{6.988493}=2.3156652$

(Cont Supplemental Table 1)

	Wis7d vs. Wis_Uninjured 2.0 fold down/upregulated genes							
	Annotation							
ProbeName	GenbankAccession	GenomicCoordinates	Description	GeneSymbol	Go	RefSeqAccession	UniGeneID	EntrezGeneID
A_44_P532352	NM_001127555	chrX:159961826-159961767	"Rattus norvegicus interleukin-1 receptor-associated kinase 1 (Irak1), mRNA [NM_001127555]"	Irak1	GO:0034142|GO:0019221|GO:0051259|GO:0042803|GO:0051092|GO:0046777|GO:0000166|GO:0016301|GO:0043406|GO:0045944|GO:0032496|GO:0043507|GO:0031663|GO:0070555|GO:0070498|GO:0016772|GO:0005149|GO:0046982|GO:0007250|GO:0034134|GO:0007254|GO:0071456|GO:0005624|GO:0005625|GO:0032088|GO:0048661|GO:0005524|GO:0007165|GO:0001959|GO:0071222|GO:0004672|GO:0004674|GO:0090370|GO:0006468|GO:0032494|GO:0045892	NM_001127555	Rn.22238	363520
A_43_P14911	NM_031512	chr3:116964524-116964465	"Rattus norvegicus interleukin 1 beta (Il1b), mRNA [NM_031512]"	Il1b	GO:0032755|GO:0014070|GO:0009408|GO:0019221|GO:0033591|GO:0042221|GO:0005615|GO:0032757|GO:0031622|GO:0030730|GO:0007611|GO:0001660|GO:0032496|GO:0033198|GO:0007613|GO:0043123|GO:0043122|GO:0010332|GO:0032355|GO:0032729|GO:0045410|GO:0032725|GO:0010193|GO:0007568|GO:0019904|GO:0030593|GO:0010243|GO:0045840|GO:0043278|GO:0005125|GO:0045086|GO:0042060|GO:0035176|GO:0008083|GO:0045833|GO:0045080|GO:0042346|GO:0002439|GO:0008285|GO:0014050|GO:0032874|GO:0033280|GO:0007204|GO:0045429|GO:0000187|GO:0006955|GO:0006954|GO:0043407|GO:0042102|GO:0043507|GO:0030141|GO:0001666|GO:0005149|GO:0043065|GO:0007584|GO:0042493|GO:0005576|GO:0006916|GO:0010829|GO:0035690|GO:0035505|GO:0010575|GO:0031982|GO:0045766|GO:0010628|GO:0001934|GO:0032611|GO:0032308|GO:0030728	NM_031512	Rn.9869	24494
A_44_P996124	NM_019178	chr5:83577410-83577469	"Rattus norvegicus toll-like receptor 4 (Tlr4), mRNA [NM_019178]"	Tlr4	GO:0005515|GO:0032755|GO:0016064|GO:0032715|GO:0002218|GO:0032757|GO:0045348|GO:0002756|GO:0002758|GO:0002755|GO:0010572|GO:0032496|GO:0032497|GO:0043123|GO:0032609|GO:0006979|GO:0031663|GO:0032689|GO:0042742|GO:0032729|GO:0032868|GO:0032728|GO:0032760|GO:0009986|GO:0032727|GO:0042535|GO:0009636|GO:0032720|GO:0032722|GO:0002224|GO:0045084|GO:0042116|GO:0005887|GO:0045087|GO:0043388|GO:0032570|GO:0045121|GO:0009897|GO:0043548|GO:0004888|GO:0042346|GO:0005886|GO:0032733|GO:0030890|GO:0032732|GO:0001875|GO:0032874|GO:0032735|GO:0002537|GO:0009617|GO:0000187|GO:0005737|GO:0006954|GO:0002282|GO:0004872|GO:0001666|GO:0014823|GO:0043065|GO:0032707|GO:0007252|GO:0032700|GO:0001530|GO:0007165|GO:0003009	NM_019178	Rn.14534	29260

	Wis_21d vs. Wis_Uninjured 2.0 fold upregulated genes							
	Annotation							
ProbeName	GenbankAccession	GenomicCoordinates	Description	GeneSymbol	Go	RefSeqAccession	UniGeneID	EntrezGeneID
A_44_P996124	NM_019178	chr5:83577410-83577469	"Rattus norvegicus toll-like receptor 4 (Tlr4), mRNA [NM_019178]"	Tlr4	GO:0005515|GO:0032755|GO:0016064|GO:0032715|GO:0002218|GO:0032757|GO:0045348|GO:0002756|GO:0002758|GO:0002755|GO:0010572|GO:0032496|GO:0032497|GO:0043123|GO:0032609|GO:0006979|GO:0031663|GO:0032689|GO:0042742|GO:0032729|GO:0032868|GO:0032728|GO:0032760|GO:0009986|GO:0032727|GO:0042535|GO:0009636|GO:0032720|GO:0032722|GO:0002224|GO:0045084|GO:0042116|GO:0005887|GO:0045087|GO:0043388|GO:0032570|GO:0045121|GO:0009897|GO:0043548|GO:0004888|GO:0042346|GO:0005886|GO:0032733|GO:0030890|GO:0032732|GO:0001875|GO:0032874|GO:0032735|GO:0002537|GO:0009617|GO:0000187|GO:0005737|GO:0006954|GO:0002282|GO:0004872|GO:0001666|GO:0014823|GO:0043065|GO:0032707|GO:0007252|GO:0032700|GO:0001530|GO:0007165|GO:0003009	NM_019178	Rn.14534	29260
A_44_P261450	NM_001105720	chr6:75730497-75730438	"Rattus norvegicus nuclear factor of kappa light polypeptide gene enhancer in B-cells inhibitor, alpha (Nfkbia), mRNA [NM_001105720]"	Nfkbia	GO:0034142|GO:0005886|GO:0042994|GO:0005634|GO:0070427|GO:0032403|GO:0010875|GO:0042802|GO:0005829|GO:0002756|GO:0005737|GO:0045638|GO:0045944|GO:0002755|GO:0031072|GO:0042127|GO:0032496|GO:0031663|GO:0031625|GO:0000060|GO:0033256|GO:0045746|GO:0051059|GO:0010745|GO:0007253|GO:0070431|GO:0006916|GO:0032088|GO:0010888|GO:0043234|GO:0032270|GO:0008139|GO:0032495|GO:0045893|GO:0019899|GO:0043330	NM_001105720	Rn.12550	25493
A_43_P14911	NM_031512	chr3:116964524-116964465	"Rattus norvegicus interleukin 1 beta (Il1b), mRNA [NM_031512]"	Il1b	GO:0032755|GO:0014070|GO:0009408|GO:0019221|GO:0033591|GO:0042221|GO:0005615|GO:0032757|GO:0031622|GO:0030730|GO:0007611|GO:0001660|GO:0032496|GO:0033198|GO:0007613|GO:0043123|GO:0043122|GO:0010332|GO:0032355|GO:0032729|GO:0045410|GO:0032725|GO:0010193|GO:0007568|GO:0019904|GO:0030593|GO:0010243|GO:0045840|GO:0043278|GO:0005125|GO:0045086|GO:0042060|GO:0035176|GO:0008083|GO:0045833|GO:0045080|GO:0042346|GO:0002439|GO:0008285|GO:0014050|GO:0032874|GO:0033280|GO:0007204|GO:0045429|GO:0000187|GO:0006955|GO:0006954|GO:0043407|GO:0042102|GO:0043507|GO:0030141|GO:0001666|GO:0005149|GO:0043065|GO:0007584|GO:0042493|GO:0005576|GO:0006916|GO:0010829|GO:0035690|GO:0035505|GO:0010575|GO:0031982|GO:0045766|GO:0010628|GO:0001934|GO:0032611|GO:0032308|GO:0030728	NM_031512	Rn.9869	24494

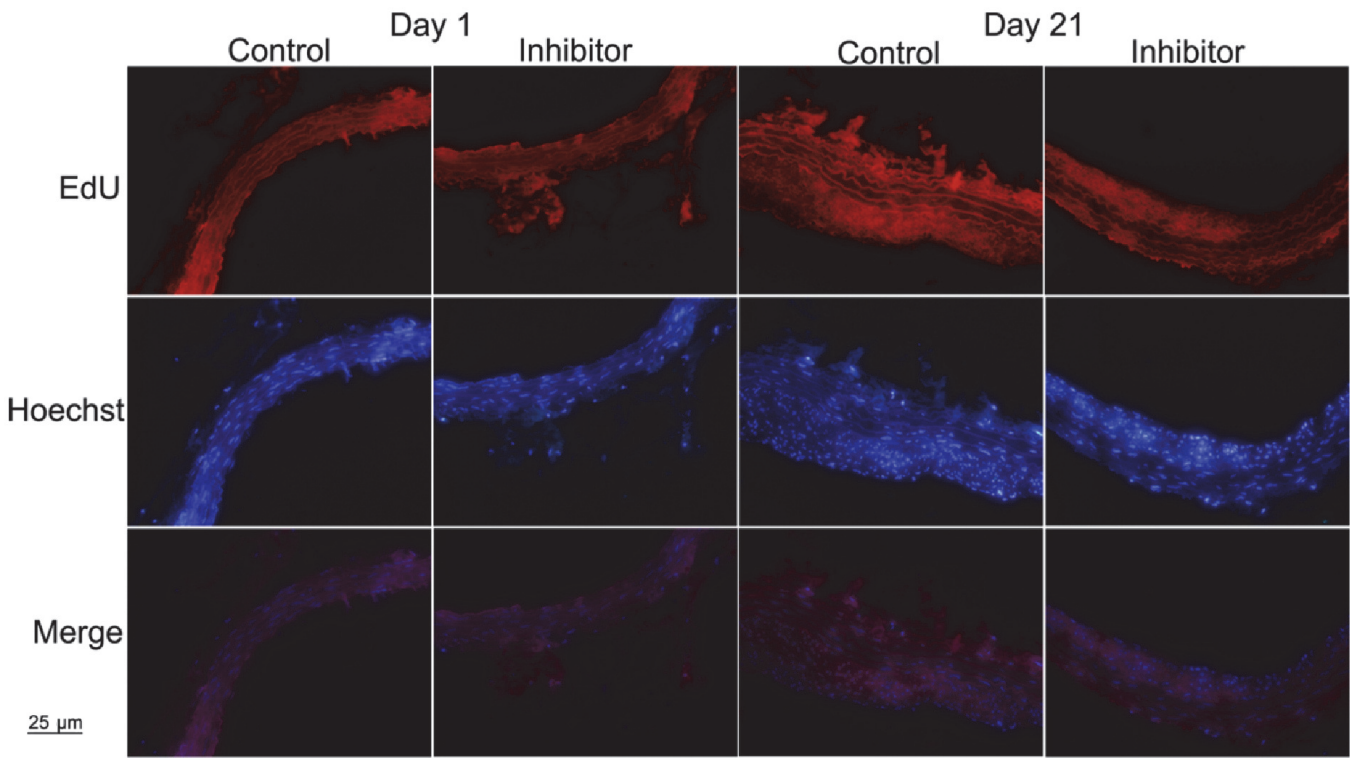

Supplemental Fig. 2.
Representative photomicrographs and quantitative results of EdU staining from injured arteries harvested at days 1 and 21 after balloon injury in the control and inhibitor groups revealed that there were almost no proliferating EdU-positive cells in the media or intima at days 1 and 21 both in the control and inhibitor groups. $n=4$.